Development of rapid and reliable cuckoo search algorithm for global maximum power point tracking of solar PV systems in partial shading condition

Khadidja BENTATA, Ahmed MOHAMMEDI and Tarak BENSLIMANE

The solar photovoltaic output power fluctuates according to solar irradiation, temperature, and load impedance variations. Due to the operating point fluctuations, extracting maximum power from the PV generator, already having a low power conversion ratio, becomes very complicated. To reach a maximum power operating point, a maximum power point tracking technique (MPPT) should be used. Under partial shading condition, the nonlinear PV output power curve contains multiple maximum power points with only one global maximum power point (GMPP). Consequently, identifying this global maximum power point is a difficult task and one of the biggest challenges of partially shaded PV systems. The conventional MPPT techniques can easily be trapped in a local maximum instead of detecting the global one. The artificial neural network techniques used to track the GMPP have a major drawback of using huge amount of data covering all operating points of PV system, including different uniform and non-uniform irradiance cases, different temperatures and load impedances. The biological intelligence techniques used to track GMPP, such as grey wolf algorithm and cuckoo search algorithm (CSA), have two main drawbacks; to be trapped in a local MPP if they have not been well tuned and the precision-transient tracking time complex paradox. To deal with these drawbacks, a Distributive Cuckoo Search Algorithm (DCSA) is developed, in this paper, as GMPP tracking technique. Simulation results of the system for different partial shading patterns demonstrated the high precision and rapidity, besides the good reliability of the proposed DCSA-GMPPT technique, compared to the conventional CSA-GMPPT.

Key words: photovoltaic system, maximum power point tracking, partial shading, cuckoo search algorithm

Kh. Bentata (e-mail: k.bentata@univ-bouira.dz) is with with Laboratory Materials and Sustainable Development (LMDD), Electrical Engineering Department, Faculty of Science and Applied Sciences, University of Bouira, Algeria.

A. Mohammedi (e-mail: mohammedi_ahmed06@yahoo.fr) is with Electrical Engineering Department, Faculty of Science and Applied Sciences, University of Bouira, Algeria and with LTII Laboratory, University of Bejaia, Algeria.

T. Benslimane (corresponding author, e-mail: tarak.benslimane@univ-msila.dz) is with Electrical Engineering Department, University of M'sila, Algeria and with SGRE Laboratory, University of Béchar, Algeria.

1. Introduction

Photovoltaic solar energy is considered to be one of the leading forms of renewable energies, which contribute in reducing the amount of electricity produced by fossil fuels. It is used in residential applications such as electricity generation for on-grid and off-grid remotely situated places such as schools, homes, clinics and buildings. It is also utilized in industrial applications as backup source of electricity for on-grid applications, and main source of electricity for off-grid remote loads, such as large-scale water pumping systems, desalination plant, radio and TV stations, lighthouse and warning light for aircraft. This is due to its numerous advantages such as being freely available, inexhaustible, widely spread, and environmental friendly [1].

Photovoltaic (PV) power array configuration is composed of a number of PV panels, which are connected in series and/or in parallel. The maximum power point (MPP) of the whole PV array is affected by environmental factors variation, such as temperature and solar irradiance. In addition, partial shading conditions due to clouds or buildings shadow makes the P-V characteristic curve more complex [1].

Because of the non-linear output power characteristics of the PV array, the improvement the efficiency of PV power generation system is realized by extracting as much as possible power from the PV modules, using usually the maximum power point tracking (MPPT) control method [2]. However, due to particular impact of different partial shading conditions (PSCs) on the non-linear PV output power-voltage (P-V) curve, the tracking of the optimal maximum power point (MPP) became a challenging task [3]. Generally, three approaches are considered to guarantee MPP tracking for partial shading conditions: (1) by retrofitting the converter, connected to PV array, with special power electronics circuitry that can recover the energy from the shaded modules [4], or (2) by employing a small converter with its own MPPT for each module in the PV array (known in the PV industry as the micro-converter) [5] or (3) by modifying the MPPT algorithm of the central converter to be more intelligent and adaptable to PSCs. The first technique is less preferable due to the additional and costly hardware that must be retrofitted into the existing system. The second approach is practically feasible for PV arrays with limited number of modules, in which individual micro-converter can be fitted under each module. However, if the system is large, the complexity and the additional costs of the electrical components increase significantly [6]. The third approach seems to be economically and technologically the most attractive technique. The MPPT algorithm can be enhanced by integrating intelligent techniques into the software, to be more adapted to the partial shading condition. Therefore, no additional hardware is needed [7].

Each one of the maximum power point tracking (MPPT) techniques has its merits and demerits [8–11]. These techniques can be classified into two main

categories, conventional techniques and the soft computing techniques. The conventional techniques such as Perturb and Observe, Incremental Conductance, Hill Climbing can track the one maximum power point (MPP) in the P-V curve of uniformly illuminated PV arrays [9,11,12]. They can easily be trapped in a Local Maximum Power Point (LMPP), and fail to track the Global Maximum Power Point (GMPP) in multi-maximum P-V curve of partially shaded PV arrays. The soft computing techniques used smart/artificial intelligent or bio-inspired technologies to recognize the GMPP of P-V curve for either uniformly illuminated or partially shaded PV array conditions [8,9,13]. The soft computing techniques used in PV MPPT applications include Particle Swarm Optimization [9,14], Gray Wolf Optimization [15], Cuckoo Search (CS), Ant Colony Optimization [16,17], Krill Herd Optimization, Firefly algorithm, artificial bee colony, Multi-Verse Optimizer, Ant Lion Optimizer, Sine Cosine Algorithm, Dragonfly Algorithm, Whale Optimization Algorithm, Moth-Flame Optimization, . . . etc. [18,19]. Most of these techniques can easily identify and track the GMPP in both cases of uniformly illuminated and partially shaded conditions of PV arrays. Nevertheless, they have two main drawbacks when being used in PV applications. The first one is associated with the dynamic or time variant GMPP position in P-V curves, in which GMPP changes its position over time, due to the solar irradiance uniformity change. In this case, most of MPP Tracking soft computing techniques identify the first GMPP at the beginning and stick around it, without recognizing any change in GMPP position. The second one is the steady state high power oscillations, due to random variables associated with all of these soft computing techniques [19].

Cuckoo search algorithm (CSA) is one of the most widely used bio-inspired optimization metaheuristic methods [20, 21]. It is characterized by relatively a small convergence time and a slight steady state error [21–23]. Compared to a variety of optimization algorithms, cuckoo search algorithm (CSA) has attracted great attention of researchers and been successfully utilized in various problems from different fields [24, 25]. This is due to its simple structure, few control parameters and implementation easiness, besides small convergence time and slight steady state error [2, 3, 23, 26–29]. However, the conventional CSA shows a main drawback of using random initialization cuckoo population of host nests, which declines the global exploration ability, deteriorates the convergence performance of conventional CSA, and causes the conventional CSA to be easy to trap into local optimum, in a multi-optimum system [30].

Several approaches have been proposed to enhance the performance of the conventional CS applied in different fields. A modified cuckoo search algorithm based on conventional CSA has been developed, in which modification comprises adding the information exchange between the top eggs or the best solutions [31]. Another approach of CSA is proposed to solve structural optimization problems, which is subsequently applied to 13 design complications reported in the spe-

cialized literature [32]. The quantum-inspired cuckoo search algorithm has been presented as an enhanced approach of CSA [33]. An improved cuckoo search algorithm has been proposed for reliability optimization problems [34]. Orthogonal learning method has been applied to enhance the performance of cuckoo search algorithm [35]. CS algorithm with hybrid strategies has been used to solve the flow shop scheduling problems [36]. An optimized hybrid method involving CS, called Cuckoo Search based on Optimally Pruned Extreme Learning Machine, has been applied to forecast solar irradiance [37]. An improved cuckoo search algorithm has been utilized for photovoltaic models parameters estimation [30]. The hybrid algorithm, based on grey wolf optimizer and cuckoo search, has been developed for parameters extraction of solar photovoltaic models [38].

The majority of enhancement efforts have been focusing on CSA applied for two types of systems. The first one is the system of static nature, where the best solutions are time-independent, whereas dynamic system has time-dependent best solutions. The second type is system with one optimum solution, whereas the multi-optimum solution systems have one global optimum solution amongst many local optimum solutions. Even for optimization problems of systems with multi-optimum and time-dependent solutions, such as MPPT of PV output power, the enhancement works of CSA have been oriented towards hybrid approaches. Therefore, to address the aforementioned drawbacks of conventional CSA, applied for a system with multi-optimum and time-dependent solutions, such as MPPT of PV output power, and to improve its rapidity and reliability performance, the Distributive Cuckoo Search Algorithm (DCSA) has been developed for PV application. In this frame, the key contributions of this paper are highlighted as follows:

- A well-tuned intelligent cuckoo search algorithm is developed to track rapidly and reliably the global maximum point of PV system under rapidly variable uniform solar irradiance and non-uniform solar irradiance (partial shading) conditions. The developed cuckoo search algorithm shows a global maximum point tracking quality with high precision, good reliability and assures a short convergence time with less power fluctuation.

- A new method is developed, based on PV system measurable electrical parameters, for estimation, characterization and differentiation of the different irradiance states for MPPT-DCSA-controlled PV system. The estimated irradiance states are : Constant uniform irradiance state, Variable uniform irradiance state and Partial shading state). The estimation approach is based on the evolution of PV array output power versus DC-DC converter duty cycle ratio.

The rest of this paper is organized as follows. In Section 2, the PV system is described and modeled. In Section 3, the impact of uniform solar irradiance

and non-uniform solar irradiance on PV array output power is highlighted. In Section 4, conventional MPPT-CSA and proposed MPPT-DCSA are presented. Simulation results are provided and discussed in Section 5. Finally, conclusions are given in Section 6.

2.   System description and modelling

The system considered in this paper is composed of PV array feeding a resistive load via MPPT-controlled boost converter (Fig. 1).
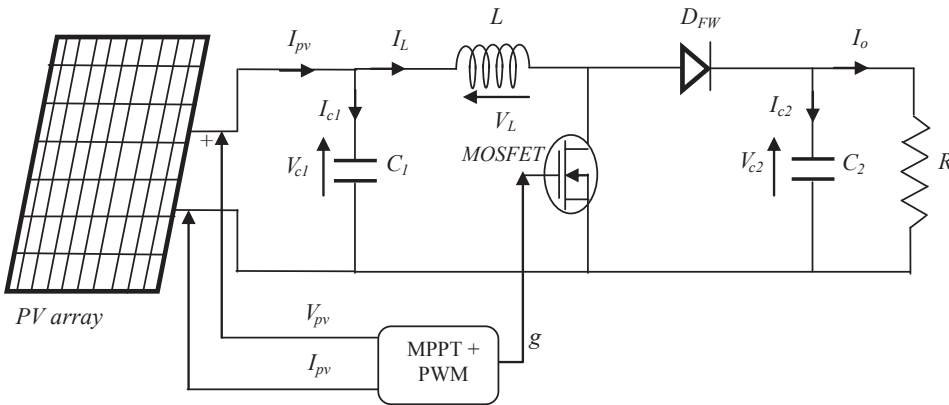
Figure 1: Schematic diagram of MPPT-controlled PV-fed boost converter

2.1.   PV cell model

Different models have been utilized to describe the electrical characteristics of PV cells, where SDM and DDM are the widely used ones, especially for electrical engineering applications [39–42]. Due to low complexity of SDM compared to DDM, it is the mostly adopted model for describing the static characteristics (I-V and P-V) of a PV cell [43]. The equivalent circuit of SDM is illustrated in Fig. 2.

This equivalent model includes a photo generated current source in parallel with a diode, a series resistor referring to the Ohmic losses associated with load current and a shunt resistor representing the leakage current [30]. Thus, the PV cell terminal current I_t can be expressed by:

$$I_t = I_{ph} - I_d - I_{sh} = I, \tag{1}$$

where I_{ph} denotes the photo generated current, I_d symbolizes the diode current, and I_{sh} represents the shunt resistor current, respectively. Moreover, in term of
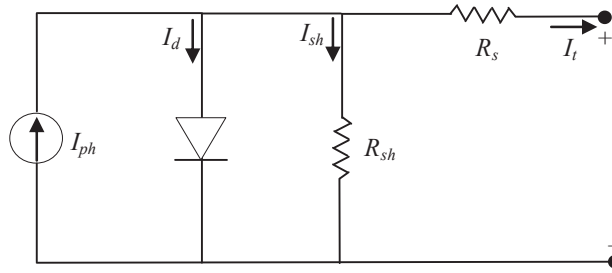
Figure 2: Equivalent circuits of a PV cell

Shockley equation, I_d can be calculated by:

$$I_d = I_{sd} \left[\exp\left(\frac{q\,(V_t + I_t R_s)}{akT} \right) - 1 \right], \tag{2}$$

where I_{sd} refers to the diode reverse saturation current, V_t represents the cell terminal voltage, R_s is the series resistance, a denotes the diode ideality factor, k is the Boltzmann constant (1.380×10^{-23} J/K), q is the electronic charge (1.602×10^{-19} C), and T is the PV cell absolute temperature in Kelvin, respectively. Moreover, via Kirchhoff's voltage law, I_{sh} can be obtained as:

$$I_{sh} = (V_t + I_t R_s)\,/R_{sh}, \tag{3}$$

where R_{sh} is the shunt resistance. Consequently, by combining Eqs. (1), (2) and (3), the I-V relationship of the SDM can be written as follows [4, 30]:

$$I_t = I_{ph} - I_{sd} \left[\exp\left(\frac{q\,(V_t + I_t R_s)}{akT} \right) - 1 \right] - (V_t + I_t R_s)\,/R_{sh}. \tag{4}$$

As a consequence, SDM has five unknown parameters, namely, I_{ph}, I_{sd}, a, R_s and R_{sh}) that can be identified based on experimental I–V data.

2.2.   PV Panel and PV array model

The PV panel contains N_{cellpar} parallel strings of N_{cellser} cells per string. So, it comes that:

$$
\begin{aligned}
I_{\text{panel}} &= \sum_{i=1}^{N_{\text{cellpar}}} I_{ti,N\text{cellpar}i} = N_{\text{cellpar}} I_t = N_{\text{cellpar}} I, \\[2mm]
V_{\text{panel}} &= \sum_{i=1}^{N_{\text{cellser}}} V_{ti,N\text{cellser}i} = N_{\text{cellser}} V_t = N_{\text{cellser}} V.
\end{aligned}
\tag{5}
$$

Similarly, the PV array containing N_{par} parallel branches of N_{ser} panels per branch; can be modeled, in case of uniform irradiance condition, by the following equation systems:

$$I_{pv} = \sum_{i=1}^{N_{par}} I_{\text{panel}i,N\text{par}i} = N_{par}I_{\text{panel}}, \quad V_{pv} = \sum_{i=1}^{N_{ser}} V_{\text{panel}i,N\text{ser}i} = N_{ser}V_{\text{panel}}. \quad (6)$$

In case of partial shading, the partially shaded string will produce a current $I_{\text{panel}i}$ of lower value compared to the uniformly illuminated strings, since the partially shaded panel will be short-circuited by the bypass diode. And since the partially shaded string and the uniformly illuminated strings are connected in parallel, the voltage across all of them V_{pv} will be the same.

2.3. Boost converter model

The boost converter is used to extract the maximum power from the PV array via duty ration control. The instantaneous values model of boost converter can be expressed by the following voltage and current equations:

$$V_{c2} = (V_{c1} - V_L)\, g + V_{c2}(1 - g) = \left(V_{pv} - V_L\right) g + V_{c2}(1 - g), \quad (7)$$

$$V_L = (V_{c1})g + (V_{c1} - V_{c2})\,(1 - g) = L\frac{\mathrm{d}I_L}{\mathrm{d}t}, \quad (8)$$

$$I_{c1} = C_1\frac{\mathrm{d}I_{c1}}{\mathrm{d}t} = I_{pv} - I_L, \quad (9)$$

$$I_{c2} = C_2\frac{\mathrm{d}I_{c2}}{\mathrm{d}t} = I_L(1 - g) - I_o. \quad (10)$$

The average values model of the boost converter can be presented by the two following equations:

$$V_{c2} = \frac{1}{1 - D}V_{c1}, \quad (11)$$

$$I_o = (1 - D)I_L = (1 - D)I_{pv}. \quad (12)$$

3. Impact of uniform solar irradiance and non-uniform solar irradiance on PV array output power

To study the behavior of PV array, associating the same parameters PV modules (Table 1) under uniform solar irradiance and non-uniform solar irradiance (partial shading), simulation tests have been carried out for various patterns of irradiance conditions (Table 2) on different PV array configurations (Fig. 3):

a) four PV modules connected in two parallel branches with two modules connected in series for each branch (2S/2P),

b) four PV modules in series (4S),

c) six PV modules connected in two parallel branches with three modules connected in series for each branch (3S/2P),

d) six PV modules connected in series (6S).

Table 1: PV module parameters (Tata Power Solar Systems TP250MBZ)

P_{max}	V_{mp}	I_{mp}	V_{oc}	I_{sc}
249	30	8.3	36.8	8.83
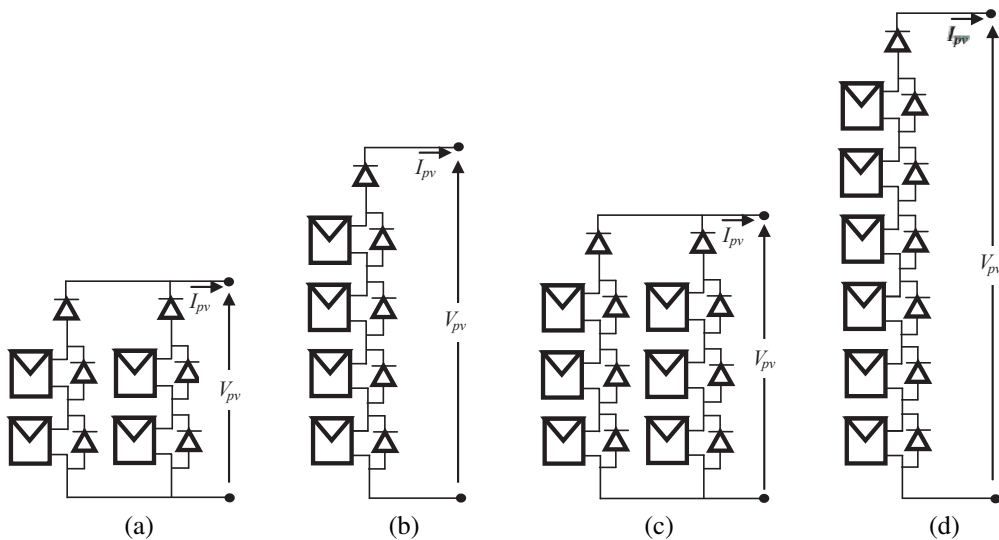
Figure 3: Configurations of PV array under partial shading, (a) two PV modules in series and two in parallels (2S/2P), (b) four PV modules in series (4S), (c) three PV modules in series and three in parallels (6S) (3S/2P), (d) six PV modules in series (6S)

Three patterns of irradiance are considered for each of the four PV array configurations. One pattern presents a uniform irradiance condition and two patters present two different partial shading conditions (Table 2).

According to simulation results of Fig. 4, some remarks have been made:

• A uniform irradiance condition is featured by the presence of only one maximum point power point.

Table 2: Irradiance (W/m^2) of each module in various patterns

	Configuration (2S/2P)			Configuration (4S)			Configuration (3S/2P)			Configuration (6S)		
Panel (M)	Pattern 1	Pattern 2	Pattern 3	Pattern 4	Pattern 5	Pattern 6	Pattern 7	Pattern 8	Pattern 9	Pattern 10	Pattern 11	Pattern 12
M-I	400	1000	600	800	1000	400	600	1000	600	200	1000	200
M-II	200	1000	200	600	1000	400	400	1000	400	200	1000	400
M-III	800	1000	600	400	1000	1000	200	1000	200	400	1000	600
M-IV	600	1000	200	200	1000	1000	1000	1000	600	400	1000	800
M-V	–	–	–	–	–	–	900	1000	400	600	1000	900
M-VI	–	–	–	–	–	–	800	1000	200	600	1000	1000

- A partial shading condition is characterized by the presence of one global maximum power point, besides many local maximum power points.

- More the number of panels having the same level of irradiance increases, more the number of maximum power points decreases and vice versa.

- More the PV panels have remarkable different irradiance levels; more the maximum power points are remarkably noticed and vice versa.

- During partial shading conditions, the maximum power points are clearly remarked in series connected PV array configurations such as 4S and 6S (Fig. 4b and Fig. 4d) compared to parallel-series connected PV array configurations such as 2S/2P and 3S/2P (Fig. 4a and Fig. 4c).

Based on the above remarks, to improve the power conversion efficiency of the PV array, it is compulsory to control the PV array output voltage in a manner to extract the maximum power. This can be a difficult task especially during partial shading conditions, where one global maximum power point emerges between many local maximum power points. Therefore, an efficient and reliable maximum power point tracking control technique should be used to determine and to force the PV system to track precisely the real global maximum power point.

Cuckoo search algorithm (CSA) is among the most widely used techniques of MPPT, for both uniform and non-uniform irradiance conditions [20]. This methodology is characterized by a better convergence and a higher proficiency, showing a minimum temporary fluctuations and a small steady state error, unlike other techniques such as Perturb and Observe and Particle Swarm Optimization [21]. Therefore, in this paper, CSA will be adopted as MPPT control technique for study and improvement purposes.

(a) 2S/2P

(b) 4S

(c) 3S/2P

(d) 6S
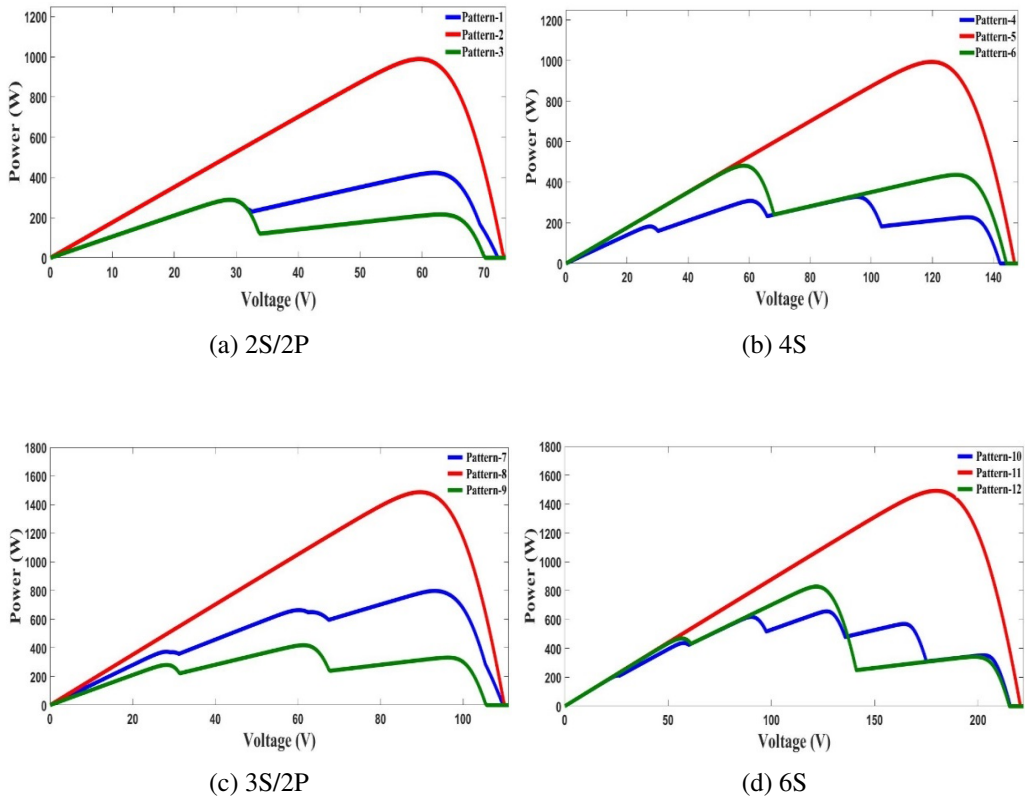
Figure 4: P–V characteristics of PV array

4. MPPT control techniques for PV system

4.1. Conventional Cuckoo search based MPPT algorithm

4.1.1. Bio-inspiration Behind Conventional Cuckoo search

Cuckoo search algorithm (CSA), inspired by the reproduction behavior of cuckoo birds, was introduced for the first time in 2009 by Xin-She Yang and Suash Deb [21]. Cuckoo birds look for a host nest to lays their eggs, so they hatch earlier. The cuckoo birds' new chicks destroy some of the host bird's eggs to increase their opportunity of survivability by keeping all the food for them. Generally, when host birds find out that the eggs in their nests are strange eggs, they destroy them or abandon the nest. Therefore, to increase the survivability of their eggs, cuckoo birds pursue a new approach via laying larger number of eggs in multiple nets.

The advantages of CSA over other bio-inspired algorithms are mainly its convergence efficiency, high accuracy, and least parametric tuning.

4.1.2.   Lévy flight

Searching for a host nest amongst many host nests is curried out randomly involving small, medium and large step sizes. Step sizes variations during host nest searching are mathematically modeled by using Lévy flight random mathematical function. In other words, Cuckoo search algorithm utilizes the Lévy flight random mathematical function to compute the random step sizes of Cuckoo search, using the following power law distribution:

$$y = l^{-\lambda}, \tag{13}$$

where l refers to the flight length and λ represents the variance. Therefore, $1 < \lambda < 3$ yields infinite variance for y. Lévy flight model yields a search steps distribution comprising small random steps and large ones. This approach proved its effectiveness in multimodal, multi-objective and nonlinear optimization problems. Generating new generation of particles $x^{(t+1)}$ by CS Lévy flight is achieved by using the following equation:

$$x_i^{(t+1)} = x_j^t + \alpha \oplus \text{Levy}(\lambda), \tag{14}$$

where i refers to the sample number, t symbolizes the iteration number and α represents the step size $\alpha > 0$. α is generally computed using the following equation [44]:

$$\alpha = \alpha_0 \left(x_j^t + x_i^t \right), \tag{15}$$

where α_0 represents the initial step change.

4.1.3.   Adaptation of conventional cuckoo search algorithm for MPPT control of PV system

One of the main applications of Cuckoo search technique in photovoltaic systems is the maximum power point tracking of PV array. In fact, under uniform irradiance condition, the PV array output Power-Voltage characteristic has a nonlinear bell shape with one maximal point. Under partial shading condition, many local maximums emerge with only one global maximum. In both cases, to maximize the PV conversion operation, the PV system must be controlled to operate under maximum power point. Therefore, a DC-DC converter, fed by the PV array, is used to control the PV array's output voltage via its duty cycle ratio in order to force the PV array to operate at the maximum power point. The cuckoo search algorithm, developed by Xin-She Yang and Suash Deb [21], can be adapted to control the DC-DC converter for MPPT of PV array system like depicted in Fig. 5. The input variables of the CS-based MPPT are PV array output voltage and current, while the output variable is the duty cycle ratio of DC-DC converter.
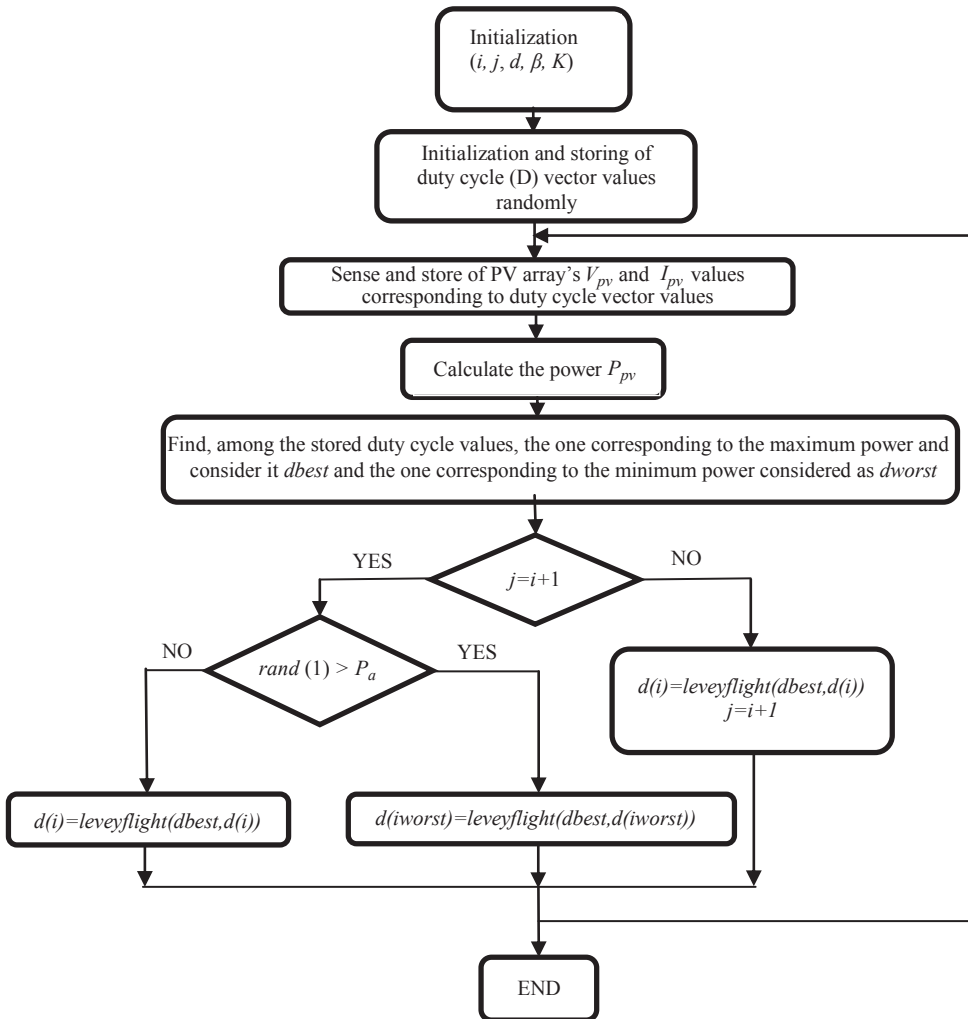
Figure 5: Flow chart of the CS algorithm for MPPT control of PV system

4.1.4.   Conventional cuckoo search algorithm Parameters tuning

CS is a nature-inspired optimization algorithm and one of the latest and most efficient ones. It is specifically inspired by some cuckoo species obligate brood parasitic behavior combined with some birds and fruit flies Lévy flight behavior. Generally, parasitic cuckoo bird searches for a nest with recently laid eggs; so, the cuckoo eggs hatch slightly before than their host bird eggs [21]. The steps of host nest searching by cuckoo bird are described by a Lévy flight mathematical model. A Lévy flight is represented mathematically as a random walk, where step sizes are extracted from Lévy flight mathematical equation.

A flowchart of the CS algorithm is shown in Fig. 5, including its significant cornerstones rules. Performance of this algorithm depends upon many factors, including population size, convergence speed, number of iterations, and information sharing efficiency in the mechanism. A small size population of particles magnifies CS algorithm defects significantly; whereas, a large size population, amplifies the computational process and convergence time. Besides that, conventional CS-based MPPT displays some drawbacks such as:

- The PV array output power oscillation during steady-state conditions due to the randomly calculated variables (duty cycle) using these bio-inspired soft computing techniques.

- The use of random initialization cuckoo population of host nests, which decreases the global exploration ability, and causes the convergence of original CSA to deteriorate and results in being easy to trap into local optimum.

- To be trapped at the first maximum power point that can be a local one, and to fail to track the real global maximum power point during partial shading conditions.

- The lack of reliable and practical detection technique of irradiance variation and partial shading conditions.

All these drawbacks will be addressed using an efficient, robust, fast and smart version of CS algorithm, which is called Distributive Cuckoo Search Algorithm (DCSA).

4.2. Proposed Distributive Cuckoo search based MPPT algorithm

4.2.1. Description

Unlike the conventional cuckoo search algorithm, based on generating a small number of randomly generated initial values particles (duty cycle values), the developed DCS is based on generating a sufficient number of initial particles with successively increasing values. Besides that, an optimized algorithm limiting the research space according to the evolution of duty cycle values and corresponding difference between maximum and minimum values of PV output powers, is introduced. This allows swapping all the particles' research space, and rapidly and smoothly reaching the steady GMP point.

4.2.2. Tuning steps of Distributive Cuckoo search based MPPT algorithm

The DCS algorithm is designed based on the following steps:

- Initialize the parameters of the DCS process using the parameters listed in Table 3.

- Start by generating and storing the duty cycle vector values (D) [0.1:0.1:0.9].

- Sense the PV array's output voltage and current (V_{pv} and I_{pv}) corresponding to duty cycle values, Store them in a vector form and Calculate the corresponding power values P_{pv}.

- Arrange the power values in ascending order from the smallest one to the biggest one [$P_1 : P_9$]. Put the corresponding duty cycle values in vector form [$d_1 : d_9$], and Calculate delta_P, delta_d, where delta_P = $(P_1 - P_9)/P_1$ and delta_d = $(d_1 - d_9)$. The given values can be divided into four different parts in terms of treatment method:

  – **the first part:** delta_d > 10^{-2} && delta_P > 20%: corresponding to the transitional regime 1.
  Update duty cycle values d using CSA where $d[d_1 : d_9]$.

  – **the second part:** delta_d > 10^{-2} && delta_P < 20%: corresponding to the transitional regime 2.
  At this part, the search process is accelerated when replacing the 3 worst duty cycle ratios corresponding to smallest power values by the best duty cycle ratio corresponding to the biggest power, and the duty cycle values $d[d_1:d_9]$ are updated using the Levy flight: $d(i) =$ leveyflight($d$best, $d(i)$), $i = 1 : 1 : 9$.

  – **the third part:** delta_d < $10 - 2$ && delta_P < 20%: corresponding to the steady state regime.
  At this part, the search process is accelerated when replacing the 6 worst duty cycle ratios corresponding to smallest power values by the best duty cycle ratio corresponding to the biggest power, and the duty cycle values $d[d_1:d_9]$ are updated using the Levy flight: $d(i) =$ leveyflight($d$best, $d(i)$), $i = 1 : 1 : 9$.

  – **the fourth part:** delta_d < 10^{-8} && delta_P > 20%: corresponding to partial shading detection.
  At this part, any changes in solar irradiance including partial shading are detected and the whole algorithm is initialized.

The basic idea behind DCSA-based MPPT can be summarized like follow:

- Relatively High-precision sweeping of the whole duty cycle ratio interval [0.1, 0.9] by applying a sufficient number of duty cycle ratios of successively increasing values with small increment (for example 9 duty ratio values increasing with increment rate of 0.1). The small variation (increment) of duty cycle ratio is adopted to minimize the transient time of the corresponding output power response. When applying a duty cycle with small increment, the PV output power will reach the steady state after a very small transient time. When the duty cycle variation (increment) is

relatively large (0.3), PV output power will reach the steady state after a relatively longer transient time.

- Replace the 3 worst duty cycle ratios corresponding to smallest power values by the best duty cycle ratio corresponding to the biggest power, and update duty cycle values using the Levy flight: $d(i) = $ leveyflight$(d$best$, d(i))$. This allows reducing the number of output powers corresponding to the duty cycle ratios from 9 output powers to 6, which limits duty cycle ratio variation, when generating new 9 values of duty cycle ratios vector using $d(i) = $ leveyflight$(d$best$, d(i))$. More the duty cycle variations become small, more the duty cycle converges to a steady state value.
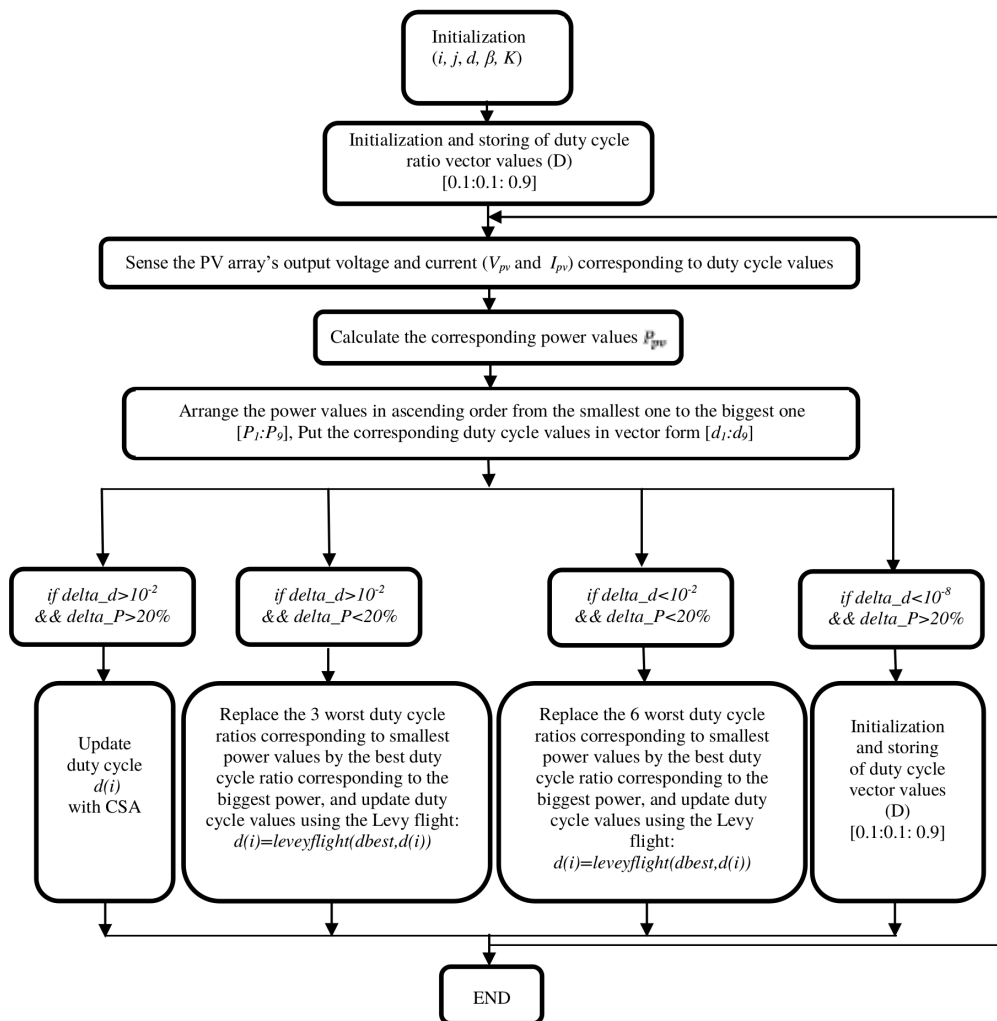
Figure 6: Flow chart of the DCS algorithm

- Replace the 6 worst duty cycle ratios corresponding to smallest power values by the best duty cycle ratio corresponding to the biggest power, and update duty cycle values using the Levy flight: $d(i) = $ leveyflight($d$best, $d(i)$). This allows reducing the number of output powers corresponding to the duty cycle ratios from 9 output powers to 3, which limits more duty cycle ratio variation, when generating new 9 values of duty cycle ratios vector using $d(i) = $ leveyflight($d$best, $d(i)$). More the duty cycle variations become small, more the duty cycle converges to a steady state value.

- Any changes in solar irradiance including partial shading are detected and the whole algorithm is initialized.

5. Simulation results of PV array under PSC

MATLAB/SIMULINK-based simulation tests are performed for GMPPT-based CSA and proposed GMPPT-based DCSA, under the three patterns of irradiance of Table 2 for each of the four PV array different configurations of Fig. 3.

The MATLAB/SIMULINK schematic diagram of the considered system, associating PV array, boost converter and resistive load, is shown in Fig. 7. DCSA, CSA and boost converter parameters are shown in Table 3. To evaluate the performances of the proposed DCS algorithm versus conventional CS algorithm, both algorithms are applied to control the boost converter as MPP techniques under three patterns of irradiance for four PV array different configurations.

Table 3: Parameters of CS and DCS algorithms and boost converter details

Particulars	Specifications
DCSA	Fraction $Pa = 0.25$, $\beta = 3/2$, $K = 0.8$. Population size (duty cycle ratio) = 9, Initial Population (duty cycle ratio) = [0.1, 0.2, 0.3, 0.4, 0.5, 0.6, 0.7, 0.8, 0.9] (Swapping the duty cycle population using successively increasing values with small increment of (0.1))
CSA	Fraction $Pa = 0.25$, $\beta = 3/2$, $K = 0.8$. Population size (duty cycle ratio) = 4, Initial Population (duty cycle ratio) = [0.1, 0.4, 0.7, 0.9] (Swapping the duty cycle population using randomly increasing values with large increment)
Boost converter	$L = 1.928$ mH, $C_1 = 10e - 6$F, $C_2 = 0.4676e - 3$F
Sampling period	$T_s = 10^{-4}$ s
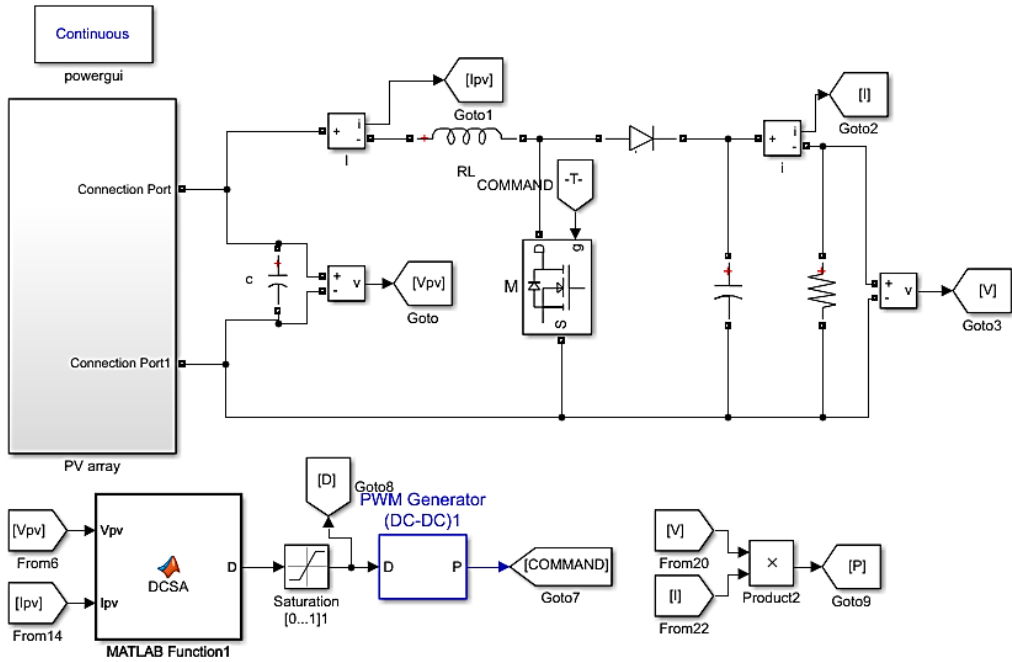
Figure 7: Simulink model of the studied system

5.1.   Simulation results of two series-two parallel PV array configuration (2S/2P)

The simulated test irradiance patterns are given in Table 2. Each pattern lasts 2 seconds, starting with first partial shading pattern (Pattern 1), where each PV panel has a different level of irradiance. Pattern 2 presents uniform irradiance condition of 1000 W/m^2 during time-period from $t = 2$ s to $t = 4$ s. The second partial shading (Pattern 3) is considered from $t = 4$ s to $t = 6$ s with same level of irradiance for each 2 PV panels of the 4 ones.

These irradiance patterns are applied on two series-two parallel PV array configuration (2S/2P) feeding a resistive load via boost converter controlled by CSA-based MPPT, and then, controlled by proposed DCSA-based MPPT. The corresponding simulation results (PV power, load voltage, load current and duty cycle waveforms) are shown in Fig. 8.

Under the first pattern (pattern 1) condition, the steady state power obtained by DCSA-MPPT is about 422.17 watts achieved after a tracking time of 0.044 seconds; whereas, the steady state power obtained by CSA-MPPT is about 422.18 watts attained after a tracking time of 0.149 seconds. DCSA-MPPT and CSA-MPPT achieve equally the power efficiency of 99.96% of the calculated reference global maximum power (422.32 Watts) corresponding to this pattern of partial shading condition. During both transient tracking and steady state, the proposed DCSA-MPPT shows less power fluctuations compared to the CSA-MPPT

(a)

(b)

(c)

(d)
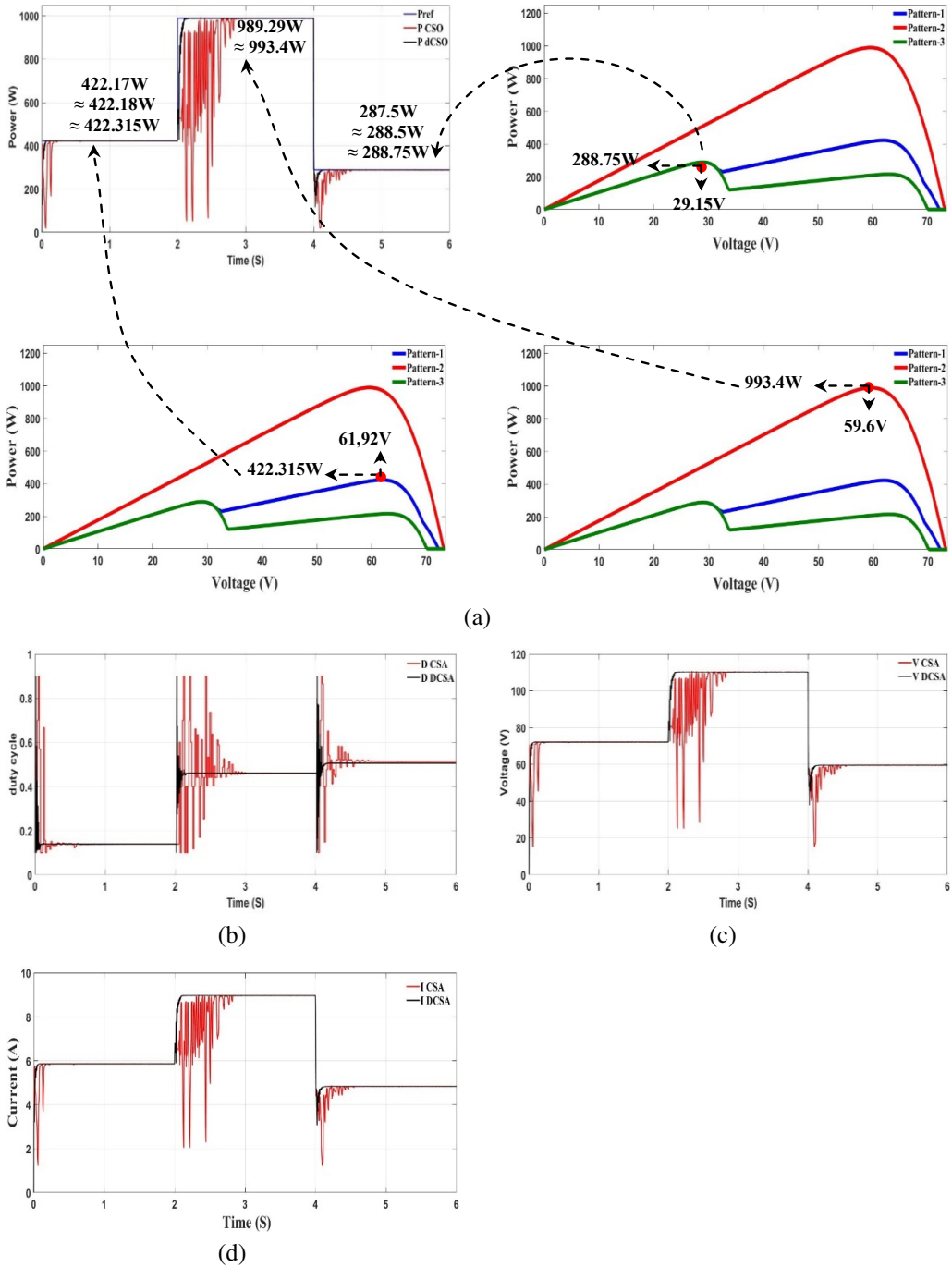
Figure 8: Simulation results of two series-two parallel PV array configuration (2S/2P) feeding a resistive load via boost converter controlled by CSA-based MPPT and by proposed DCSA-based MPPT

(Fig. 8a). Therefore, DCSA-MPPT allows reaching the actual GMPP almost
3.5 times faster than CSA-MPPT with much less power oscillations. The duty cy-
cle updating indicates that DCSA-MPPT can detect and converge to GMPP faster
than CSA-MPPT (Fig. 8b). The corresponding voltage and current are presented
in (Fig. 8c) and (Fig. 8d).

Under second pattern (pattern 2) condition, both DCSA-MPPT and CSA-
MPPT allows getting 989.29 watts of power after a transitory tracking time of
0.073 seconds for the first control technique and 0.820 seconds for the second
one. Under this uniform irradiance, DCSA-MPPT and CSA-MPPT both achieved
energy efficiency of 99.58% of the full rated power (993.4 Watts), calculated
for uniform irradiance condition of 1000 W/m^2. The corresponding PV array
output voltage is equal to 59.6 V, which is tightly close to the maximum power
point voltage of PV array calculated according to PV module parameters of
Table 1 ($V_{mp} = 2 \times 30 = 60$ V). As regards the transient period of tracking, it is
characterized by huge power fluctuations for CSA-MPPT control technique, and
insignificant ones for DCSA-MPPT control technique. Besides that, the proposed
DCSA-MPPT achieved a transient tracking period more than eleven times shorter
than the conventional CSA-MPPT (Fig. 8a). The duty cycle ratios corresponding
to both CSA-MPPT and DCSA-MPPT converge to the same value of 0.46, with
shorter convergence time and less fluctuations of DCSA-MPPT duty cycle ratio
compared to CSA-MPPT duty cycle ratio (Fig. 8b). The corresponding load
voltage and current are presented in Fig. 8c and Fig. 8d.

For third pattern (pattern 3) condition, the CSA-MPPT outperformed DCSA-
MPPT by an insignificant slight difference in terms of energy efficiency with
99.91% compared to 99.56% of the calculated reference global maximum power
(288.75 W Watts), by scoring a power of 288.5 Watts for CSA-MPPT and 287.5
Watts for DCSA-MPPT. In terms of tracking speed, DCSA-MPPT achieved a
transient tracking time more than five times shorter than transient tracking time
scored by CSA-MPPT (Fig. 8a). The corresponding duty cycle ratio, voltage and
current are depicted in Figs. 8b, 8c and 8d.

5.2. Simulation results of four series PV array configuration (4S)

The simulated test irradiance patterns (pattern 4, pattern 5 and pattern 6) given
in Table 2 are applied successively during 2 seconds of time for each pattern.
These irradiance patterns are applied on four series PV array configuration (4S)
feeding a resistive load via boost converter controlled by CSA-based MPPT, and
then, controlled by proposed DCSA-based MPPT. The corresponding simulation
results (PV power, load voltage, load current and duty cycle waveforms) are
depicted in Fig. 9.

During the partial shading condition of pattern 4, the power obtained by
DCSA-MPPT is about 327.68 Watts with transient tracking time of 0.061 seconds;

(a)

(b)

(c)

(d)
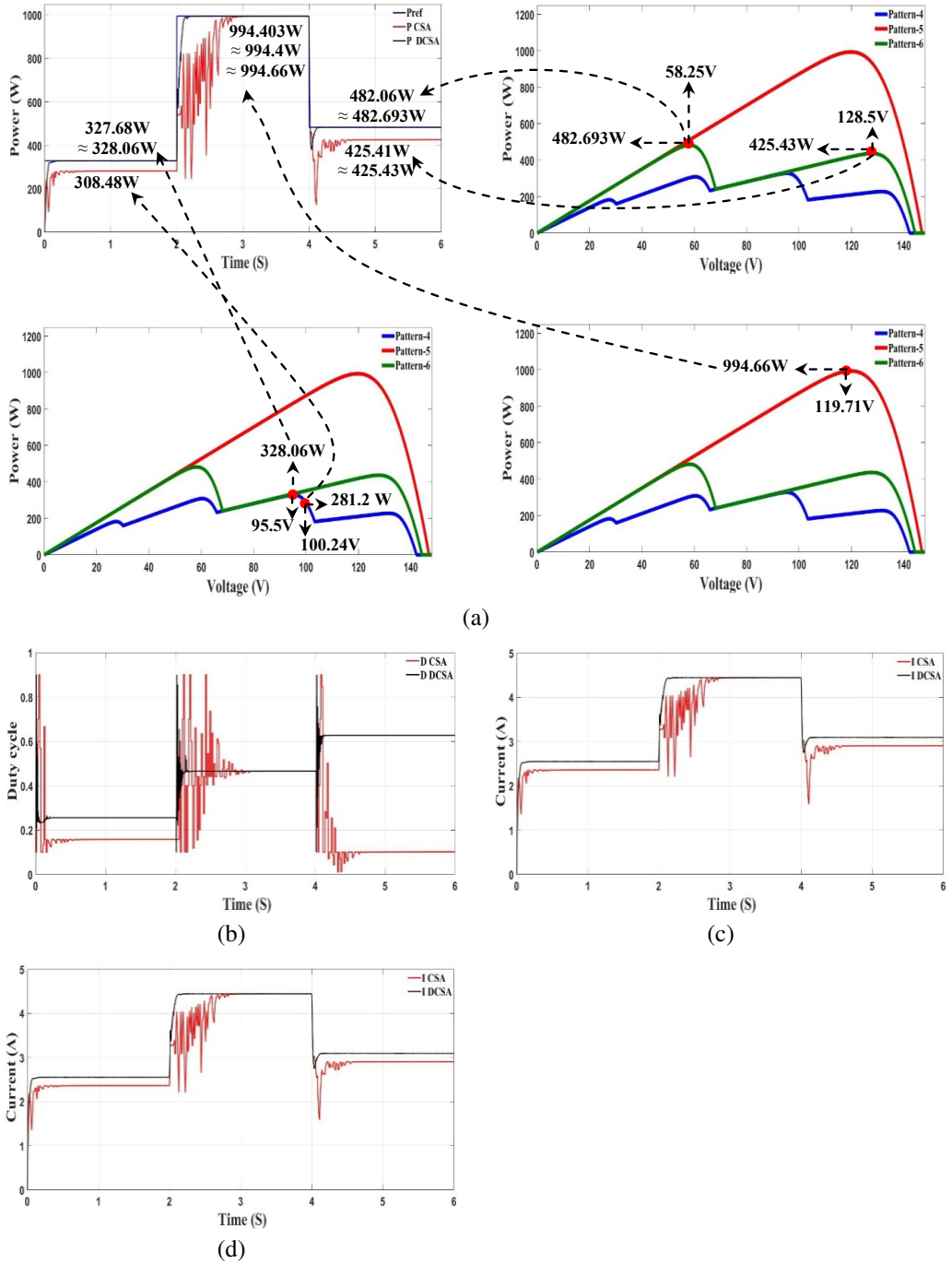
Figure 9: Simulation results of four series PV array configuration (4S) feeding a resistive load via boost converter controlled by CSA-based MPPT and by proposed DCSA-based MPPT

while the power obtained by CSA-MPPT is around 281.2 Watts with a transient tracking time of 0.166 seconds. The proposed DCSA-MPPT has achieved a power efficiency of 99.88% of the calculated reference global maximum power (328.06 Watts) corresponding to this pattern of partial shading condition. As regard, the CSA-MPPT, it tracked the GMPP of 328.06 Watts with lower efficiency of 85.716% (Fig. 9a). The tracking accuracy (efficiency) is decreased because of using CSA with limited population size (duty cycle ratio) of 4 particles, which corresponds to the population size commonly chosen for conventional CSA. To increase the tracking accuracy (efficiency), the population size (duty cycle ratio) should be increased, but the transient tracking time will be increased too, which decreases the tracking speed. DCSA-MPPT duty cycle ratio and CSA-MPPT duty cycle ratio have different values, which are successively 0.255 and 0.158.

As regard the partial shading condition of pattern 6, when the PV system is controlled by DCSA-MPPT, it succeeded to track the actual Global MPP of 482.693 Watts by achieving a MPP of 482.06 Watts, which is 99.868% of the actual GMPP. When the same PV system is controlled by CSA-MPPT, it was trapped in the Local MPP of 425.43 W by achieving 425.41 Watts, which is 88.132% of the actual Global MPP of 482.693 Watts (Fig. 9a). Hence, DCSA-MPPT duty cycle ratio and CSA-MPPT duty cycle ratio have different values, which are successively 0.626 and 0.102.

According to these results of both partial shading conditions of pattern 4 and pattern 6, it is quite clear that DCSA-MPPT is highly efficient and reliable in GMPP tracking compared to CSA-MPPT. The load voltage and current, corresponding to both partial shading conditions of pattern 4 and pattern 6, are displayed in Fig. 9c and Fig. 9d.

Under uniform irradiance condition of pattern 5, where only one MPP exists, both DCSA-MPPT and CSA-MPPT succeeded in scoring a MPP of 994.4 Watts, which is 99.97% of the actual GMPP of 994.66 Watts. The corresponding PV array output voltage is equal to 119.71 V, which is tightly close to the maximum power point voltage of PV array calculated according to PV module parameters of Table 1 ($V_{mp} = 4 \times 30 = 120$ V). As regards the transient tracking times, they are 0.089 seconds for DCSA-MPPT and 0.702 seconds for CSA-MPPT, in which the PV system experienced significant power fluctuation when controlled by CSA-MPPT compared to DCSA-MPPT (Fig. 9a). The duty cycle ratios corresponding to both CSA-MPPT and DCSA-MPPT converge to the same value of 0.465, with shorter convergence time and less fluctuations of DCSA-MPPT duty cycle ratio compared to CSA-MPPT duty cycle ratio (Fig. 9b). The corresponding load voltage and current are illustrated in Fig. 9c and Fig. 9d.

5.3. Simulation results of three series-two parallel PV array configuration (3S/2P)

For partial shading condition of pattern 7, DCSA-MPPT successfully tracked the GMPP with an efficiency of 99.94% of the 797.7 Watts actual GMPP, by achieving a power of 797.3 Watts in a transient tracking time of 0.046 seconds. For

the same partial shading, CSA-MPPT failed for the third time to track the GMPP with an efficiency of 93.93% by being trapped in a local MPP of 749.3 Watts in a transient tracking time of 0.165 seconds (Fig. 10a). The corresponding duty cycle ratios converge to different values, which are 0.222 for DCSA-MPPT and 0.158 for CSA-MPPT, with significantly shorter convergence time and less fluctuation observed on DCSA-MPPT duty cycle ratio compared to CSA-MPPT duty cycle ratio (Fig. 10b).

The load voltage and current, corresponding to partial shading conditions of pattern 7, are presented in Fig. 10c and Fig. 10d.

With the uniform irradiance of pattern 8, although DCSA-MPPT and CSA-MPPT tracked the 1486 Watts maximum power point with high efficiency of 99.96% by recording a power of 1485.5 Watts, DCSA-MPPT is nine times faster with a transient tracking time of 0.084 seconds versus 0.776 seconds for CSA-MPPT (Fig. 10a). Therefore, the duty cycle ratios corresponding to both DCSA-

(a)   (b)

(c)   (d)
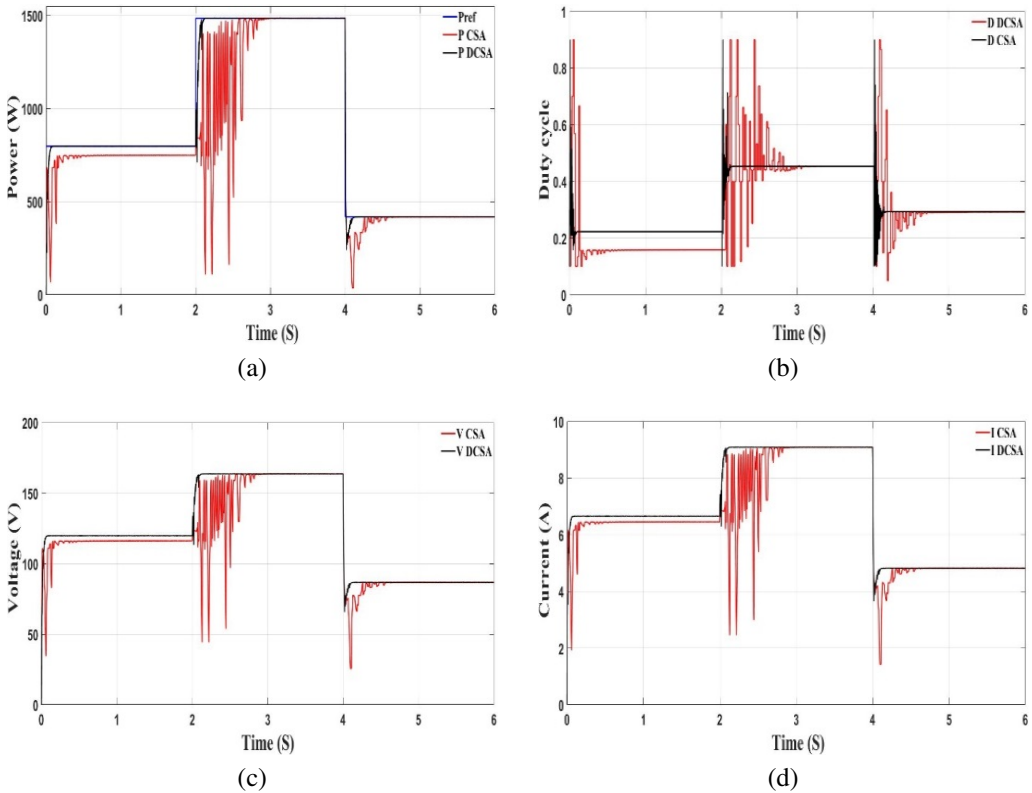
Figure 10: Simulation results of three series-two parallel PV array configuration (3S/2P) feeding a resistive load via boost converter controlled by CSA-based MPPT and by proposed DCSA-based MPPT

MPPT and CSA-MPPT converged approximately to the same value of 0.453, with convergence time difference (Fig. 10b). The load voltage and current, corresponding to uniform irradiance of pattern 8, are presented in Fig. 10c and Fig. 10d.

Same remarks have been observed regarding partial shading condition of pattern 9. Both DCSA-MPPT and CSA-MPPT reached the 418.4 Watts GMPP with power efficiency of 99.96% by recording a power of 418.24 Watts. However, DCSA-MPPT achieved this power in a transient tracking time five times shorter than CSA-MPPT, with less power fluctuation (Fig. 10a). Therefore, the duty cycle ratios corresponding to both DCSA-MPPT and CSA-MPPT converged approximately to the same value (0.293 for DCSA-MPPT and 0.292 for CSA-MPPT), with convergence time difference (Fig. 10b). The load voltage and current, corresponding to partial shading condition of pattern 9, are shown in Fig. 10c and Fig. 10d.

5.4.   Simulation results of six series PV array configuration (6S)

Under partial shading condition of pattern 10, the power obtained by using DCSA-MPPT was 656.45 Watts after transient tracking time of 0.078 seconds; while, the power obtained by using CSA-MPPT was 565.44 Watts after a transient tracking time of 0.22 seconds. In other words, the DCSA-MPPT attained the Global MPP by achieving 99.88 % of the 657.2 Watts actual GMPP; whereas, CSA-MPPT is trapped in one of the Local MPPs with 86.03% of the actual GMPP power (Fig. 11a). Therefore, after transient tracking time, the duty cycle ratios of DCSA-MPPT and CSA-MPPT showed two different steady states of 0.398 for DCSA-MPPT duty cycle ratio and 0.155 for CSA-MPPT duty cycle ratio (Fig. 11b). The load voltage and current, corresponding to partial shading conditions of pattern 10, are presented in Fig. 11c and Fig. 11d.

With a uniform irradiance condition pattern like pattern 11, one only actual MPP will characterize the PV array's Power-Voltage curve. In pattern 11 case, this MPP corresponds to 1491.8 Watts power. With DCSA-MPPT, the PV output power reaches 99.91% of actual MPP with 1490.55 Watts, after a transient tracking time of 0.089 seconds. With CSA-MPPT, the PV output power attains 99.67% of actual MPP with 1486.90 Watts, after a transient tracking time of 0.632 seconds. So, while both of the MPPT techniques succeeded in tracking the GMPP, DCSA-MPPT technique demonstrated high tracking speed (more than 7 times faster) compared to CSA-MPPT technique (Fig. 11a). The corresponding duty cycle ratios are depicted in Fig. 11b, while the corresponding load voltage and current are presented in Fig. 11c and Fig. 11d.

Same remarks have been observed during partial shading condition of pattern 12. DCSA-MPPT achieved 99.882% of actual GMPP power of 828.92 Watts by scoring 827.95 Watts. CSA-MPPT reached 99.886% of actual GMPP power of 828.92 Watts by scoring 827.98 Watts. Thus, both MPPT techniques success-

fully tracked the actual GMPP, with the difference of tracking speed in which DCSA-MPPT demonstrated higher performance versus CSA-MPPT (Fig 11a. The duty cycle ratios corresponding to partial shading condition of pattern 12 are illustrated in Fig. 10b, while the corresponding load voltage and current are displayed in Fig. 11c and Fig. 11d.
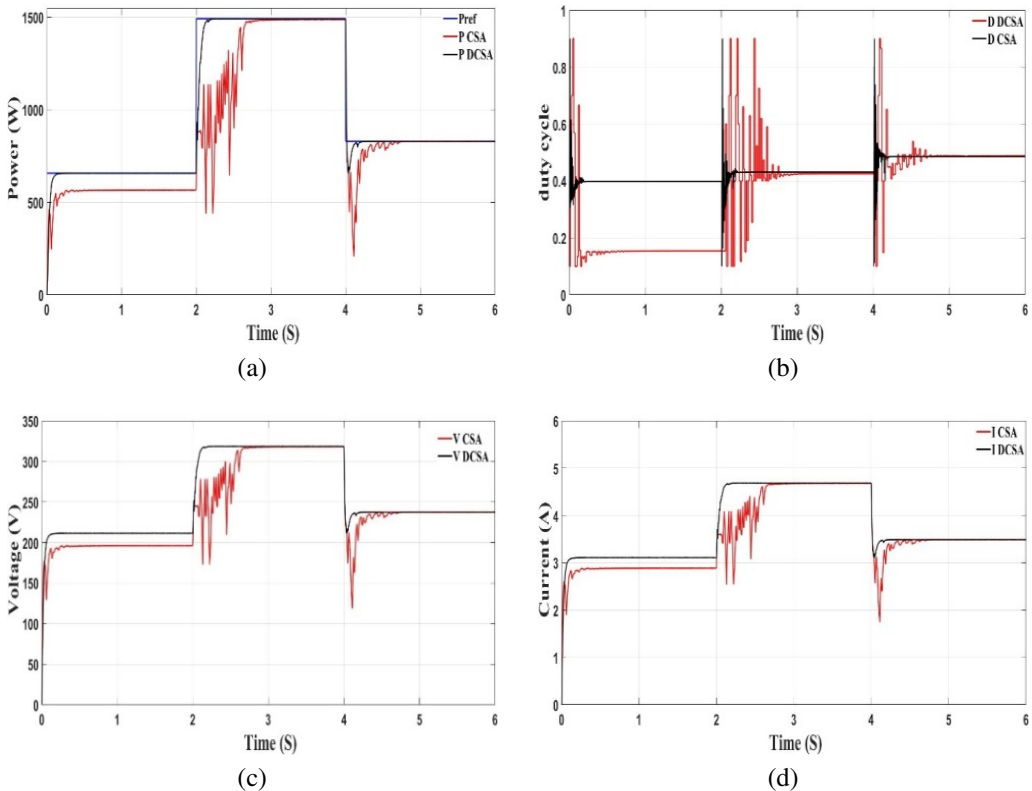
Figure 11: Simulation results of six series PV array configuration (6S) feeding a resistive load via boost converter controlled by CSA-based MPPT and by proposed DCSA-based MPPT

To evaluate the performance of the proposed DCSA-MPPT versus the conventional CSA-MPPT, simulation results of PV system controlled by DCSA-MPPT are compared quantitatively and qualitatively to the simulation results of the same PV system controlled by CSA-MPPT for the same PV array configurations and the same patterns of irradiance (Fig. 12, Table 4 and Table 5).

It is quite clear that over 12 cases of irradiance patterns, the conventional CSA-MPPT control technique succeeded in tracking the actual GMPP in 8 cases (pattern 1, pattern 2, pattern 3, pattern 5, pattern 8, pattern 9, pattern 11, pattern 12), and failed for the 4 other cases (pattern 4, patter 6, patter 7 and pattern 10),

Table 4: Quantitative comparison of DCSA-MPPT and CSA-MPPT performances for 12 patterns of irradiance

PV configuration	Irradiance pattern	Tracking algorithm	PV output Power (W)	Voltage (V)	Current (A)	Duty cycle	Tracking time (s)	GM located	Maximum power (W) determined from P-V curve	Efficiency (%)
2S/2P	Pattern 1	DCSA	422.17	72.065	5.8582	0.1398	0.044	Yes	422.32	99.96
		CSA	422.18	72.063	5.8579	0.1393	0.149	Yes		99.96
	Pattern 2	DCSA	989.29	110.25	8.962	0.46	0.073	Yes	993.4	99.58
		CSA	989.29	110.25	8.962	0.495	0.820	Yes		99.58
	Pattern 3	DCSA	287.5	59.48	4.836	0.506	0.085	Yes	288.75	99.56
		CSA	288.5	59.56	4.482	0.514	0.470	Yes		99.91
4S	Pattern 4	DCSA	327.68	128.513	2.559	0.255	0.061	Yes	328.06	99.884
		CSA	281.2	119.045	2.362	0.158	0.166	No		85.716
	Pattern 5	DCSA	994.403	223.755	4.439	0.465	0.089	Yes	994.66	99.974
		CSA	994.4	223.755	4.439	0.465	0.702	Yes		99.973
	Pattern 6	DCSA	482.06	155.87	3.092	0.626	0.085	Yes	482.693	99.868
		CSA	425.41	146.428	2.905	0.102	0.379	No		88.132
3S/2P	Pattern 7	DCSA	797.3	119.795	6.655	0.222	0.046	Yes	797.7	99.949
		CSA	749.3	116.135	6.452	0.158	0.165	No		93.932
	Pattern 8	DCSA	1485.5	163.55	9.086	0.453	0.084	Yes	1486	99.966
		CSA	1485.5	163.55	9.086	0.453	0.776	Yes		99.966
	Pattern 9	DCSA	418.24	86.754	4.820	0.293	0.087	Yes	418.4	99.961
		CSA	418.21	86.750	4.819	0.292	0.470	Yes		99.954
6S	Pattern 10	DCSA	656.45	211.28	3.107	0.398	0.078	Yes	657.2	99.885
		CSA	565.44	196.08	2.883	0.153	0.22	No		86.037
	Pattern 11	DCSA	1490.55	318.36	4.682	0.431	0.089	Yes	1491.8	99.916
		CSA	1486.90	317.98	4.676	0.425	0.632	Yes		99.671
	Pattern 12	DCSA	827.95	237.28	3.489	0.488	0.089	Yes	828.92	99.882
		CSA	827.98	237.28	3.489	0.485	0.534	Yes		99.886

like shown in Fig. 12a, Fig. 12b and Table 4. Besides that, when CSA-MPPT control technique succeeded in tracking the actual GMPP, the transient tracking time (convergence time) was relatively long (Fig. 12c and Table 4). On the contrary,

(a)

(b)

(c)
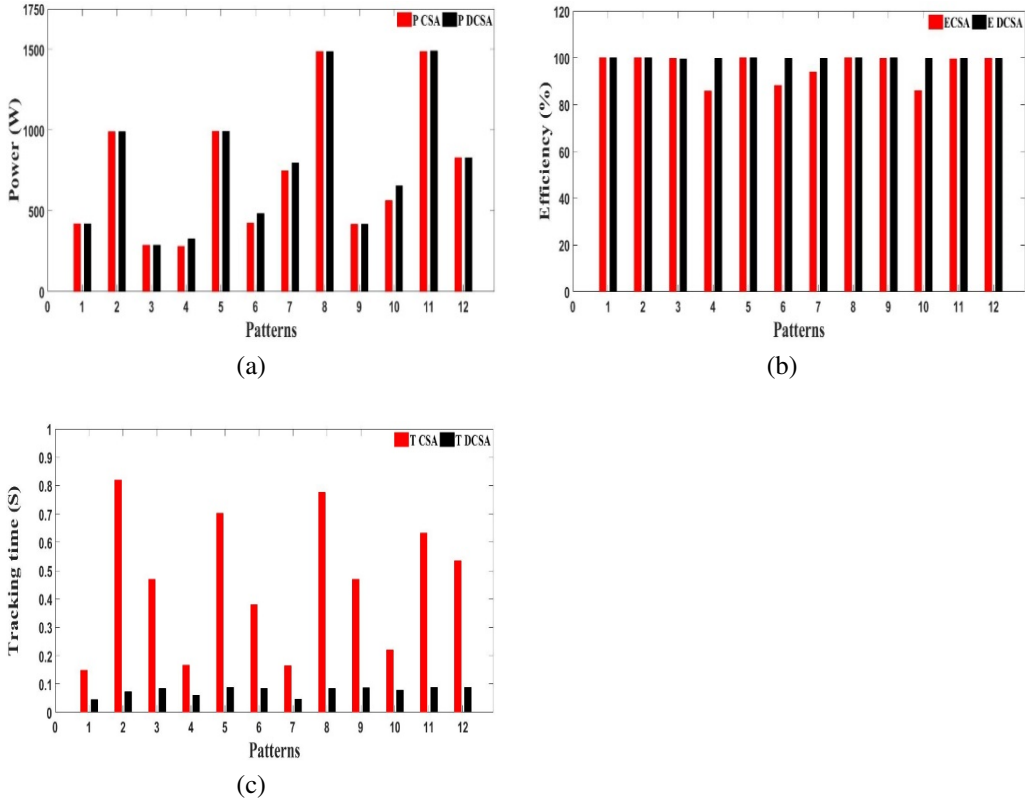
Figure 12: PV output power, Efficiency and MPP tracking time of DCSA-MPPT and CSA-MPPT for 12 patterns of irradiance: (a) power, (b) efficiency, (c) tracking time

the proposed DCSA-MPPT control technique succeeded in tracking the actual GMPP in all 12 cases, with shorter transient tracking time (convergence time) (Fig. 12a, Fig. 12b, Fig. 12c and Table 4).

Table 5: Quantitative comparison of DCSA-MPPT and CSA-MPPT performances for 12 patterns of irradiance

Parameters	CSA	DCSA
Tracking success	Good	Excellent
Tracking speed	Moderate	Fast
Iterations	More	Less
Initial particles	Dependent	Independent
Number of particles	4	9/6/3

6.   Conclusion

Power efficiency enhancement of PV systems, already having low power conversion ratio, have been the main research axis of many research works. Therefore, PV arrays output power maximization was a key factor for improvement of PV systems Power efficiency. As PV array output power is strongly dependent on solar irradiance value and uniformity level and uniformity, which are time-dependent factors, makes PV power maximization very complicated. Many control techniques have been developed for maximum power point tracking of PV array output power in both conditions of uniform and non-uniform solar irradiance. MPPT based on Cuckoo search algorithm is one of these techniques, which proved a good performance in terms of precision and rapidity, especially in uniform solar irradiance condition. Even though, under partial shading condition of PV array, it demonstrated a low level of reliability in tracking the actual global maximum power point, by being trapped in local maximum ones. To overcame these drawbacks, distributive cuckoo search algorithm have been developed, in this paper, for maximum power point tracking of PV array under both conditions of uniform and non-uniform conditions. The developed MPPT-DCSA revealed a high level of precision and reliability, high tracking speed and low fluctuating output power of PV array.

References

[1] Zhao Zhuoli, Runting Cheng, Baiping Yan, Jiexiong Zhang, Zehan Zhang, Mingyu Zhang, and Loi Lei Lai: A dynamic particles MPPT method for photovoltaic systems under partial shading conditions. *Energy Conversion and Management*, **220** (2020), 113070, DOI: 10.1016/j.enconman.2020.113070.

[2] Nabil A. Ahmed and Masafumi Miyatake: A novel maximum power point tracking for photovoltaic applications under partially shaded insolation conditions. *Electric Power Systems Research*, **78**(5), (2008), 777–784, DOI: 10.1016/j.epsr.2007.05.026.

[3] Liqun Liu, Xiaoli Meng, and Chunxia Liu: A review of maximum power point tracking methods of PV power system at uniform and partial shading. *Renewable and Sustainable Energy Reviews*, **53** (2016), 1500–1507, DOI: 10.1016/j.rser.2015.09.065.

[4] Yanzhi Wang, Xue Lin, Younghyun Kim, Naehyuck Chang, and Massoud Pedram: Enhancing efficiency and robustness of a photovoltaic power

system under partial shading. *Thirteenth International Symposium on Quality Electronic Design* (ISQED), Santa Clara USA, (2012), 592–600, DOI: 10.1109/ISQED.2012.6187554.

[5] RICARDO ORDUZ, JORGE SOLÓRZANO, MIGUEL ÁNGEL EGIDO, and EDUARDO ROMÁN: Analytical study and evaluation results of power optimizers for distributed power conditioning in photovoltaic arrays. *Progress in Photovoltaics: Research and Applications*, 21(3), (2013), 359–373, DOI: 10.1002/pip.1188.

[6] KASHIF ISHAQUE and ZAINAL SALAM: A review of maximum power point tracking techniques of PV system for uniform insolation and partial shading condition. *Renewable and Sustainable Energy Reviews*, **19** (2013), 475–488, DOI: 10.1016/j.rser.2012.11.032.

[7] JUBAER AHMED and ZAINAL SALAM: A critical evaluation on maximum power point tracking methods for partial shading in PV systems. *Renewable and Sustainable Energy Reviews*, **47** (2015), 933–953, DOI: 10.1016/j.rser.2015.03.080.

[8] ALI M. ELTAMALY: *Performance of MPPT techniques of photovoltaic systems under normal and partial shading conditions*. Advances in Renewable Energies and Power Technologies, vol. 1, Solar and Wind Energies, I. Yahyaoui, 2018, Elsevier, Chapter 4, 115–161.

[9] ALI M. ELTAMALY: Performance of smart maximum power point tracker under partial shading conditions of photovoltaic systems. *Journal of Renewable and Sustainable Energy*, **7**(4), (2015), 043141, DOI: 10.1063/1.4929665.

[10] A. TALHA, H. BOUMAARAF, and O. BOUHALI: Evaluation of maximum power point tracking methods for photovoltaic systems. *Archives of Control Sciences*, **21**(2), (2011), 151–165.

[11] HEGAZY REZK and ALI M. ELTAMALY: A comprehensive comparison of different MPPT techniques for photovoltaic systems. *Solar Energy*, **112** (2015), 1–11, DOI: 10.1016/j.solener.2014.11.010.

[12] S. LYDEN and M.E. HAQUE: Maximum power point tracking techniques for photovoltaic systems: A comprehensive review and comparative analysis. *Renewable and Sustainable Energy Reviews*, **52** (2015): 1504–1518, DOI: 10.1016/j.rser.2015.07.172.

[13] ZAINAL SALAM, JUBAER AHMED, and BENNY S. MERUGU: The application of soft computing methods for MPPT of PV system: A technological and status review. *Applied Energy*, **10**7 (2013), 135–148, DOI: 10.1016/j.apenergy.2013.02.008.

[14] HASSAN M.H. FARH, MOHAMED F. OTHMAN, and ALI M. ELTAMALY: Maximum power extraction from grid-connected PV system. *Saudi Arabia Smart Grid* (SASG), (2017), 1–6, DOI: 10.1109/SASG.2017.8356498.

[15] SEYEDALI MIRJALILI, SEYED MOHAMMAD MIRJALILI, and ANDREW LEWIS: Grey Wolf optimizer. *Advances in Engineering Software*, **69** (2014), 46–61, DOI: 10.1016/j.advengsoft.2013.12.007.

[16] SABRINA TITRI, CHERIF LARBES, KAMAL YOUCEF TOUMI, and KARIMA BENATCHBA: A new MPPT controller based on the ant colony optimization algorithm for photovoltaic systems under partial shading conditions. *Applied Soft Computing*, **58** (2017), 465–479, DOI: 10.1016/j.asoc.2017.05.017.

[17] LIAN LIAN JIANG, DOUGLAS L. MASKELL, and JAGDISH C. PATRA: A novel ant colony optimization-based maximum power point tracking for photovoltaic systems under partially shaded conditions. *Energy and Buildings*, **58** (2013), 227–236, DOI: 10.1016/j.enbuild.2012.12.001.

[18] LIAN LIAN JIANG, R. SRIVATSAN, and DOUGLAS L. MASKELL: Computational intelligence techniques for maximum power point tracking in PV systems: A review. *Renewable and Sustainable Energy Reviews*, **85** (2018), 14–45, DOI: 10.1016/j.rser.2018.01.006.

[19] ALI M. ELTAMALY and HASSAN M.H. FARH: Dynamic global maximum power point tracking of the PV systems under variant partial shading using hybrid GWO-FLC. *Solar Energy*, **177** (2019), 306–316, DOI: 10.1016/j.solener.2018.11.028.

[20] JUBAER AHMED and ZAINAL SALAM: A maximum power point tracking (MPPT) for PV system using cuckoo search with partial shading capability. *Applied Energy*, **119** (2014), 118–130, DOI: 10.1016/j.apenergy.2013.12.062.

[21] XIN-SHE YANG and SUASH DEB: Cuckoo search via Lévy flights. *2009 World Congress on Nature & Biologically Inspired Computing* (NaBIC), Coimbatore, India (2009), 210–214, DOI: 10.1109/NABIC.2009.5393690.

[22] JUBAER AHMED and ZAINAL SALAM: A soft computing MPPT for PV system based on cuckoo search algorithm. *4th International Conference on Power Engineering, Energy and Electrical Drives*, Istanbul, Turkey, (2013), 558–562, DOI: 10.1109/PowerEng.2013.6635669.

[23] AHMED A. EL BASET, A. EL HALIM, NAGGAR H. , and AHMED A. EL SATTAR: A comparative study between perturb and observe and cuckoo search algorithm for maximum power point tracking. *21st International Middle East*

Power Systems Conference (MEPCON), Cairo, Egypt, (2019), 716–723, DOI: 10.1109/MEPCON47431.2019.9008210.

[24] FILIPPO SPERTINO and JEAN SUMAILI AKILIMALI: Are manufacturing I–V mismatch and reverse currents key factors in large photovoltaic arrays? *IEEE Transactions on Industrial Electronics*, **56**(11), (2009), 4520–4531, DOI: 10.1109/TIE.2009.2025712.

[25] M. DRIF, P.J. PEREZ, J. AGUILERA, and J.D. AGUILAR: A new estimation method of irradiance on a partially shaded PV generator in grid-connected photovoltaic systems. *Renewable Energy*, **33**(9), (2008), 2048–2056, DOI: 10.1016/j.renene.2007.12.010.

[26] BIDYADHAR SUBUDHI and RASESWARI PRADHAN: A comparative study on maximum power point tracking techniques for photovoltaic power systems. *IEEE Transactions on Sustainable Energy*, **4**(1), (2012), 89–98, DOI: 10.1109/TSTE.2012.2202294.

[27] KASHIF ISHAQUE and ZAINAL SALAM: A comprehensive MATLAB Simulink PV system simulator with partial shading capability based on two-diode model. *Solar Energy*, **85**(9), (2011), 2217–2227, DOI: 10.1016/j.solener.2011.06.008.

[28] MOHAMED I.MOSAAD, M. OSAMA ABED EL-RAOUF, MAHMOUD A. AL-AHMAR, and FAHD A. BANAKHER: Maximum power point tracking of PV system based cuckoo search algorithm; review and comparison. *Energy Procedia*, **162** (2019), 117–126, DOI: 10.1016/j.egypro.2019.04.013.

[29] BO YANG, JINGBO WANG, XIAOSHUN ZHANG, TAO YU, WEI YAO, HONGCHUN SHU, FANG ZENG, and LIMING SUN: Comprehensive overview of meta-heuristic algorithm applications on PV cell parameter identification. *Energy Conversion and Management*, **208** (2020), 112595, DOI: 10.1016/j.enconman.2020.112595.

[30] TONG KANG, JIANGANG YAO, MIN JIN, SHENGJIE YANG, and THANHLONG DUONG: A novel improved cuckoo search algorithm for parameter estimation of photovoltaic (PV) models. *Energies*, **11**(5), (2018), 1060, DOI: 10.3390/en11051060.

[31] S. WALTON, O. HASSAN, K. MORGAN, and M.R. BROWN: Modified cuckoo search: a new gradient free optimisation algorithm. Chaos, *Solitons & Fractals*, **44**(9), (2011), 710718, DOI: 10.1016/j.chaos.2011.06.004.

[32] AMIR HOSSEIN GANDOMI, XIN-SHE YANG, and AMIR HOSSEIN ALAVI:
Cuckoo search algorithm: a metaheuristic approach to solve structural op-
timization problems. *Engineering with Computers*, **29**(1), (2013), 17–35,
DOI: 10.1007/s00366-011-0241-y.

[33] ABDESSLEM LAYEB: A novel quantum inspired cuckoo search for knapsack
problems. *International Journal of Bio-Inspired Computation*, **3**(5), (2011),
297–305, DOI: 10.1504/IJBIC.2011.042260.

[34] EHSAN VALIAN, SAEED TAVAKOLI, SHAHRAM MOHANNA, and ATIYEH
HAGHI: Improved cuckoo search for reliability optimization problems.
Computers & Industrial Engineering, **64**(1), (2013), 459–468, DOI:
10.1016/j.cie.2012.07.011.

[35] XIANGTAO LI, JIANAN WANG, and MINGHAO YIN: Enhancing the perfor-
mance of cuckoo search algorithm using orthogonal learning method.
Neural Computing and Applications, **24**(6), (2014), 1233–1247, DOI:
10.1007/s00521-013-1354-6.

[36] HUI WANG, WENJUN WANG, HUI SUN, ZHIHUA CUI, SHAHRYAR RAHNA-
MAYAN, and SANYOU ZENG: A new cuckoo search algorithm with hybrid
strategies for flow shop scheduling problems. *Soft Computing*, **21**(15),
(2017), 4297–4307, DOI: 10.1007/s00500-016-2062-9.

[37] WANG JIANZHOU, HE JIANG, YUJIE WU, and YAO DONG: Forecasting solar
radiation using an optimized hybrid model by cuckoo search algorithm.
Energy, **81** (2015), 627–644, DOI: 10.1016/j.energy.2015.01.006.

[38] WEN LONG, SHAOHONG CAI, JIANJUN JIAO, MING XU, and TIEBIN WU:
A new hybrid algorithm based on grey wolf optimizer and cuckoo search for
parameter extraction of solar photovoltaic models. *Energy Conversion and
Management*, **203** (2020), 112243, DOI: 10.1016/j.enconman.2019.112243.

[39] DIEGO OLIVA, AHMED A. EWEES, MOHAMED ABD EL AZIZ, ABOUL ELLA
HASSANIEN, and MARCO PERÉZ-CISNEROS: A chaotic improved artificial
bee colony for parameter estimation of photovoltaic cells. *Energies*, **10**(7),
(2017), 865, DOI: 10.3390/en10070865.

[40] XIAOFANG YUAN, YUQING HE, and LIANGJIANG LIU: Parameter extrac-
tion of solar cell models using chaotic asexual reproduction optimiza-
tion. *Neural Computing and Applications*, **26**(5), (2015), 1227–1239, DOI:
10.1007/s00521-014-1795-6.

[41] XIAOFANG YUAN, YONGZHONG XIANG, and YUQING HE: Parameter extrac-
tion of solar cell models using mutative-scale parallel chaos optimization

algorithm. *Solar Energy*, **108** (2014), 238–251, DOI: 10.1016/j.solener.2014.07.013.

[42] ALIREZA ASKARZADEH and ALIREZA REZAZADEH: Artificial bee swarm optimization algorithm for parameters identification of solar cell models. *Applied Energy*, **102** (2013), 943–949, DOI: 10.1016/j.apenergy.2012.09.052.

[43] SANTHAN KUMAR CHERUKURI and SRINIVASA RAO RAYAPUDI: Enhanced grey wolf optimizer based MPPT algorithm of PV system under partial shaded condition. *International Journal of Renewable Energy Development*, **6**(3), (2017), 203–212, DOI: 10.14710/ijred.6.3.203-212.

[44] ADEEL FEROZ MIRZA, QIANG LING, M. YAQOOB JAVED, and MAJAD MANSOOR: Novel MPPT techniques for photovoltaic systems under uniform irradiance and Partial shading. *Solar Energy*, **184** (2019), 628–648, DOI: 10.1016/j.solener.2019.04.034.